

Large eddy simulation of a transverse hydrogen jet in supersonic crossflow

Alexey Troshin*, Vladimir Vlasenko** and Vladimir Sabelnikov***

*Central Aerohydrodynamic Institute, Zhukovsky, Russia

Moscow Institute of Physics and Technology, Dolgoprudny, Russia

ai-troshin@yandex.ru

**Central Aerohydrodynamic Institute, Zhukovsky, Russia

Moscow Institute of Physics and Technology, Dolgoprudny, Russia

vlasenko.vv@yandex.ru

***Central Aerohydrodynamic Institute, Zhukovsky, Russia

ONERA, Palaiseau, France

vladimir.sabelnikov@onera.fr

Abstract

Simulations of a transverse hydrogen jet injection in supersonic air flow are presented carried out using TsAGI in-house finite volume code *zFlare*. Hybrid SST-IDDES model with SLA subgrid length scale was employed. The computational mesh contained 22 million cells. In the paper, vortex structure of the flow is analyzed, combustion zones are detected and compared to the experimental data, separation zone length is determined, and hydrogen flow penetration depth is estimated. At least qualitative correspondence to the experiment is found, and for certain flow characteristics, quantitative improvement is obtained as compared with the data available in the literature.

1. Introduction

One of the major challenges of high speed aircraft propulsion system design is effective fuel mixing and combustion process during a short residence time inside the engine. Transverse injection of fuel through a wall-mounted nozzle is a common and reliable injection scheme that provides rapid mixing of fuel with air and deep jet penetration into a supersonic flow. This flow is a topic of many studies and publications, see e.g. [1].

Due to complex flow structure (Fig. 1) involving near-wall and free turbulence, several separation zones, shock wave interaction and unsteady effects, RANS approach is not reliable enough for predicting such flow [2].

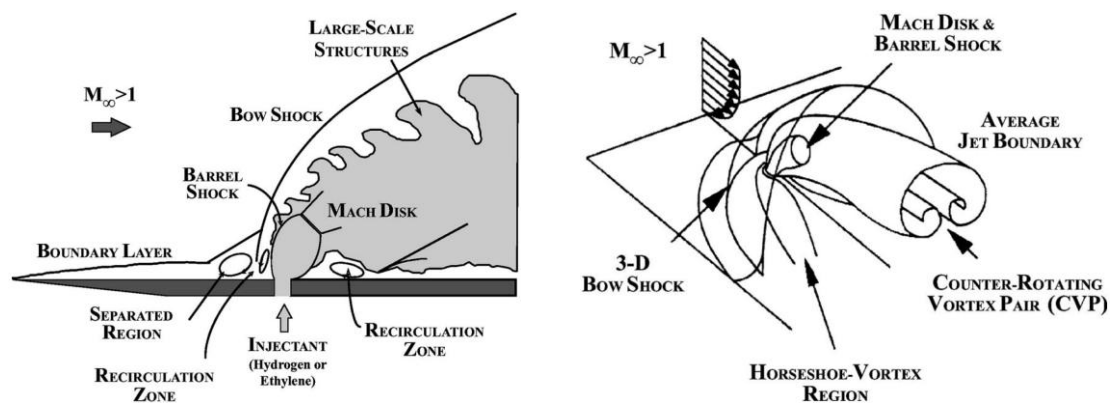


Figure 1: Flow structure of transverse injection into a supersonic crossflow, taken from [3]

Instead, there are attempts to large- and detached-eddy simulations of transverse injection into a supersonic crossflow [4, 5, 6]. These studies are aimed both at understanding LES capabilities for this type of flows and at revealing new flow physics unavailable from experiments. Reacting flow poses additional difficulties concerning the influence of chemistry model, numerical resolution of heat release zones and consideration of turbulence-combustion interaction, not all of which are solved reliably at present.

The main goal of the present research is to validate DES technology implemented in TsAGI in-house code *zFlare* based on *ZEUS-S3pp* [7]. This code is designed for combustion chamber simulations, so correct modeling of fuel injection is an essential part for the overall solution reliability.

The paper is organized as follows. In Section 2, flow configuration and regime taken for numerical simulation is specified. In Section 3, numerical setup is given including hybrid model, computational domain and mesh, boundary conditions and numerical method. In Section 4, computational results are compared to the experimental data and discussed. After that, the conclusions follow.

2. Flow configuration and regime

An experiment [3, 8] is simulated in which a flat plate with high speed solenoid valve attached is placed in supersonic air stream, see Fig. 1. The valve ensures almost constant injection flow rate during the test time period. Expansion tube is used to reach the desired high-enthalpy flow regime with steady flow time $\tau \sim 270 \mu\text{s}$. Short test period allows considering the plate as cold and take its temperature equal to 288 K. Injector diameter is $d_j = 2 \text{ mm}$ with underexpanded hydrogen jet. The injector is placed $l = 50 \text{ mm}$ downstream of the plate leading edge. The undisturbed boundary layer is laminar and reaches thickness of 0.75 mm at the starting point of interaction with hydrogen. Flow regime summary is presented in the Table 1.

Table 1: Flow regime summary

	Value
Inflow Mach number	3.38 ± 0.04
Injected hydrogen Mach number	1.0
Inflow static temperature	1290 K
Injected hydrogen static temperature	246 K
Inflow static pressure	32.4 kPa
Injected hydrogen static pressure	490 kPa
Reynolds number based on $l = 50 \text{ mm}$	2.2×10^5
Jet-to-freestream momentum flux ratio	1.4

From the experiment, instantaneous and time-averaged Schlieren photographs are available as well as OH planar laser-induced fluorescence images. From the data, hydrogen penetration depth, coherent structure characteristics, and molecular mixing zones can be determined.

3. Numerical setup

For numerical simulation, 3D box computational domain was used (Fig. 2). It was filled with Cartesian mesh containing 22 million cells. Domain of interest with constant longitudinal and lateral mesh spacing covers the box defined as $[-5d_j, 10d_j] \times [0, 10d_j] \times [-5d_j, 5d_j]$. Coordinate system origin is placed at the injector center, x is undisturbed flow direction, y is wall-normal direction, and z axis is directed spanwise. In wall-normal direction, first cell above the wall has height $2 \times 10^{-5} \text{ m}$. A detailed mesh view is depicted in Fig. 3.

At the supersonic inlet as well as at the upper boundary, undisturbed flow parameters were specified. In the region covering $-25d_j < x < -7.5d_j$, turbulence model source terms were switched off for the laminar boundary layer to form on the plate. Downstream the $x = -7.5d_j$ section, turbulent boundary layer was modeled by means of wall function approach [9] on the lower boundary. Lateral boundaries were periodic. At the outlet, the solution was extrapolated outside the computational domain. Finally, round injector surface was not tracked by mesh lines. Instead, the injector was modeled by means of a composite boundary condition at which the convective fluxes associated with hydrogen flow were multiplied by the surface fraction occupied by the injector.

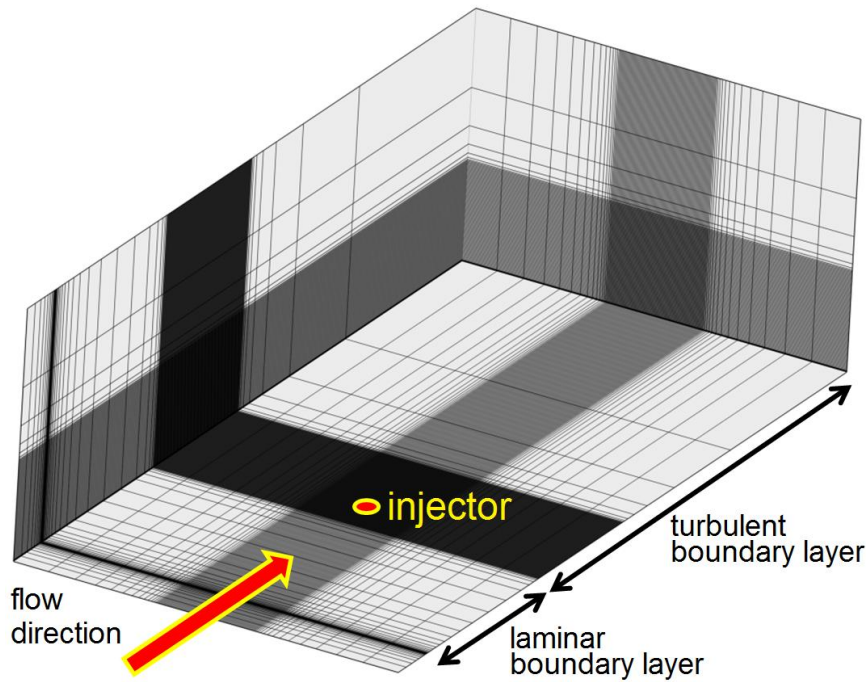
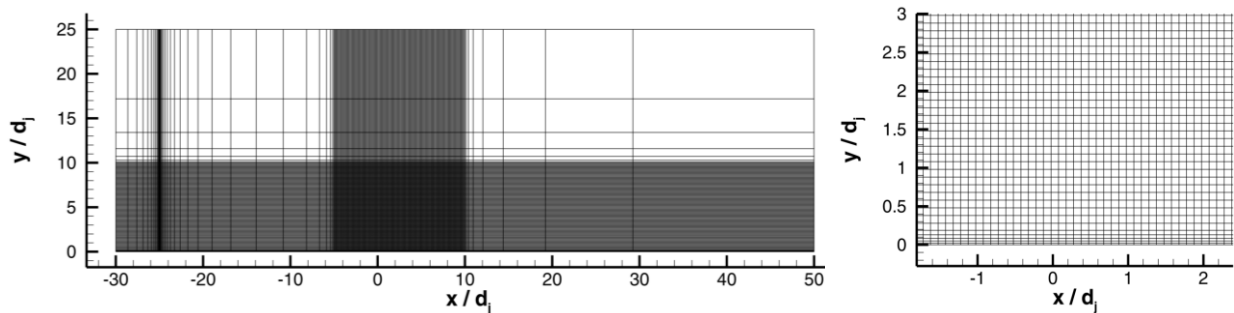


Figure 2: Computational domain scheme

Figure 3: Mesh in xy plane and injection region (each second node is shown)

The computations were carried out using TsAGI in-house code *zFlare* based on *ZEUS-S3pp* [7]. This code is designed for 3D flow computations with non-equilibrium chemical reactions using RANS, URANS, and DES approaches. In the present research, the problem was solved using SST-IDDES hybrid model [10] with shear layer adapted subgrid length scale [11]. To reduce the numerical dissipation of the scale resolving simulation, WENO5 scheme along mesh lines with MP limiting [12] was used. Exact iterative Godunov Riemann solver was employed to calculate the numerical fluxes at the cell faces. Time marching was performed using 2nd order explicit time scheme accelerated with original Fractional time stepping technique (FTS) [13]. According to the tests conducted, FTS typically provides 10×–30× acceleration compared to a conventional global time step.

The computation was started from a preliminary flow field obtained in steady RANS SST computation. Statistically steady state was allowed to establish during the time interval $\Delta t_1 = 200d_j / U_j$, where $U_j = 1250$ m/s is the approximate hydrogen velocity at the injector exit. After that, the flowfield was averaged during the interval $\Delta t_2 = 75d_j / U_j$. 256 CPU cores of an HPC cluster were used. Several runs were performed on the “Lomonosov” supercomputer [14].

4. Results

In Fig. 4, comparison of the instantaneous flow field (static temperature) with a Schlieren photograph from an experiment is shown. One can see the agreement on the structure of the flow and the characteristic size of large eddies on the windward side of the mixing layer.

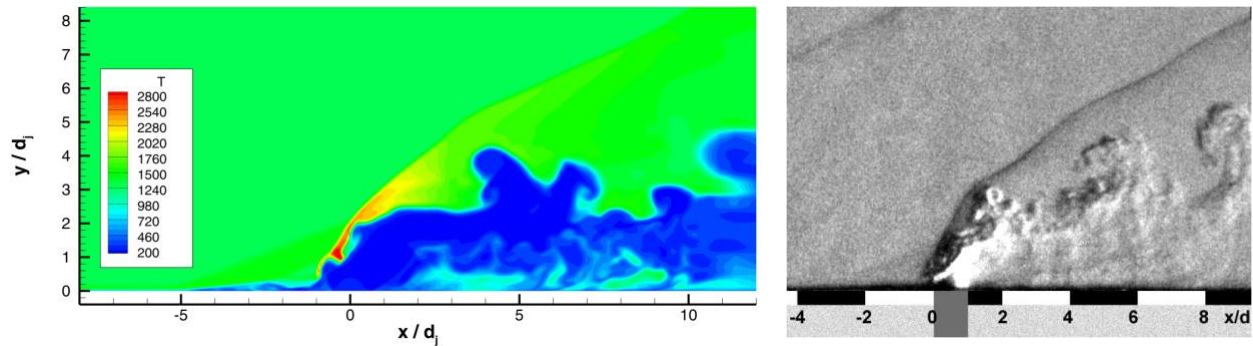


Figure 4: Comparison of instantaneous static temperature field (left) from numerical simulation with an experimental Schlieren photograph (right) taken from [8]

In Fig. 5, the computational and experimental fields of OH radical mass fraction are depicted. Both in the experiment and in the simulation, active combustion is observed on the windward side of the mixing layer, while on its leeward side there are almost no reactions. In the separation zone upstream of the injector, the intensity of combustion observed in the experiment is low, while in the simulation it is almost completely zero. One can find the flame front structures scale in the simulation to be larger than in experiment, probably due to insufficient mesh resolution in this region.

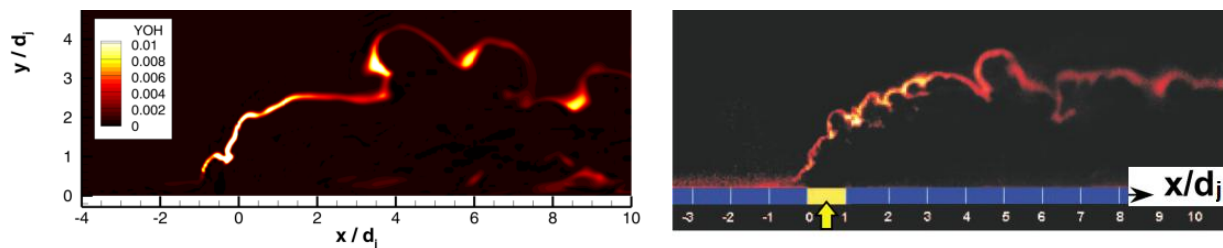


Figure 5: Comparison of instantaneous OH mass fractions obtained in the simulation (left) and in the experiment (right) taken from [8]

The vortex structure of the flow obtained in the simulation is shown in Fig. 6 by means of the Q -criterion isosurface [15, 16]. Individual organized vortices attached to the plate and as well as strong vorticity layer are visible on the leeward side of the mixing layer. At the same time, the vortices are larger on the windward side, and the Q -criterion does not detect them. The formation of small-scale vorticity in this region is probably inhibited by the proximity of the bow shock near the mixing layer. High level of vorticity is also evident in the horseshoe vortex formed around the injection zone.

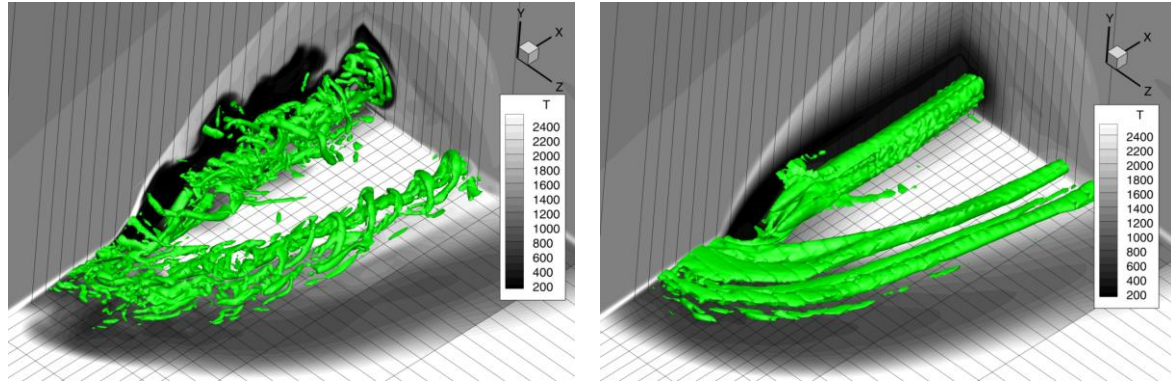


Figure 6: Vortex structure of the flow: instantaneous (left) and time-averaged (right) Q -criterion isosurfaces

An analysis of the separation zone length upstream of the injector revealed the discrepancies compared to the experiment. As can be seen in Fig. 7, the separation zone length in the simulation is $5.5d_j$, while in the experiment it is about $2d_j$. To understand the reason for such a difference, additional simulation was performed with further reduction of numerical dissipation. It was done by zonal switch to central difference schemes for convective fluxes according to the blending function proposed in [17]. The minimal weight of upwind WENO5 scheme was set to $\sigma = 0.25$ to avoid numerical instabilities. In this simulation (Fig. 8), greatly reduced separation length was found which matched the experiment with 10% accuracy.

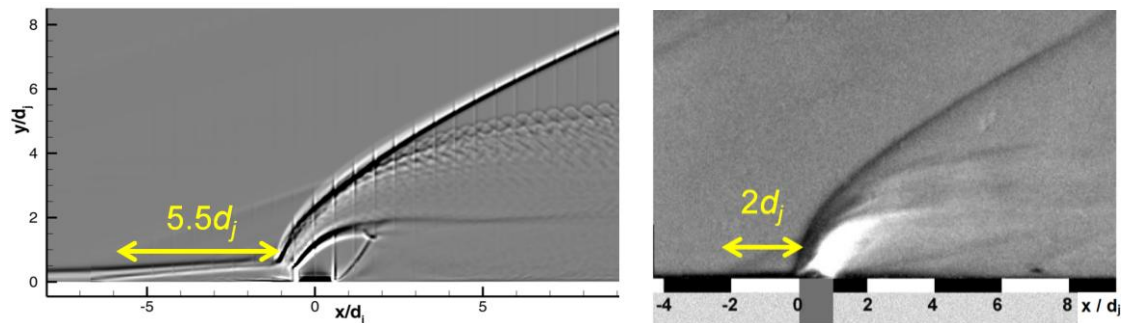


Figure 7: Separation zone length analysis. Present “standard” simulation (left), time-averaged Schlieren photograph (right) taken from [8]

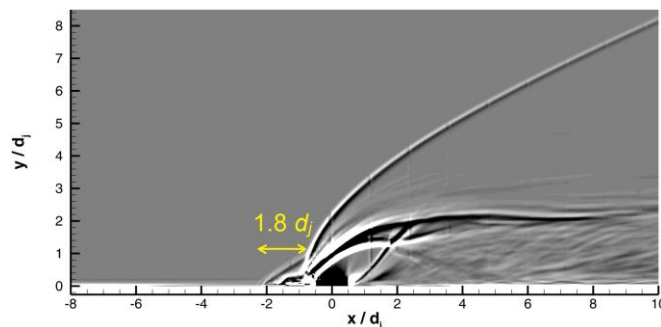


Figure 8: Separation zone length analysis. Present “reduced dissipation” simulation

The main difference between the “standard” and “reduced dissipation” simulations near the separation zone was found at the wall where turbulence levels turned out to be different (Fig. 9). In the “standard” simulation, transition to turbulence starting at the $x = -7.5d_j$ section, is delayed, which causes separation zone to be partially laminar. As a consequence, its length grows. On the other hand, transition to turbulence in the “reduced dissipation” simulation is more intensive due to higher values of resolved velocity gradients, so separation zone becomes fully turbulent. It makes its length significantly closer to the experiment.

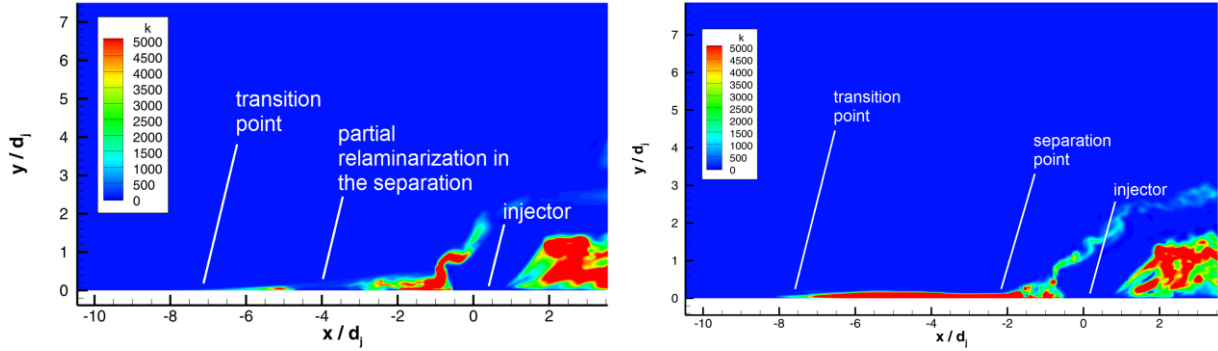


Figure 9: Separation zone length analysis. Transition to turbulence upstream the separation zone, “standard” simulation (left) and “reduced dissipation” simulation (right)

Finally, estimation was made of the hydrogen jet penetration depth into the air stream. In Table 2, the values of the wall-normal coordinate are presented where the mass fraction of hydrogen 0.01 is detected in $x = 7.5d_j$ cross-section. Compared to RANS data [7] and DES data [6], the present simulation demonstrates a closer correspondence to the experimental data, the error being within 10%.

Table 2: Hydrogen penetration depth in $x = 7.5d_j$ cross-section

	Depth, y / d_j
Experiment [3, 8]	5.3
RANS data [7]	3.9
DES data [6]	4.3
Present IDDES	5.0

5. Conclusions

The scale-resolving technology implemented in *zFlare* code is validated in the simulations of a transverse hydrogen jet in supersonic crossflow. At least qualitative correspondence to the experiment is obtained, and for certain flow characteristics, quantitative improvement is obtained as compared with the data available in the literature. Stable computation and parallel operation on 10^2 - 10^3 CPU cores of an HPC cluster is demonstrated. It can be concluded that the code is ready to solve the problems concerning the physical aspects of combustion chamber flows.

Considering the discrepancies found in the test, it is planned to further investigate the influence of the numerical scheme. As is shown in the preliminary computation employing central difference schemes, it can change the flow pattern significantly. It is also reasonable to calibrate the key constants of the hybrid SST-IDDES model in order to tune the numerical dissipation level correctly. Finally, the effect of time derivative approximation on the stability and accuracy of the solution will be studied in the future.

Acknowledgments

The research was supported by the Ministry of Education and Science of Russian Federation (“megagrant”, agreement No. 14.G39.31.0001).

The authors are grateful to S. Bahnă for mesh generation and preliminary code testing.

References

- [1] Sun, M., H. Wang, and F. Xiao. 2019. Jet in supersonic crossflow. Springer. 284 p.
- [2] Tam, C.-J., R.A. Baurle, and M.R. Gruber. 1999. Numerical study of jet injection into a supersonic crossflow. *AIAA Paper* 1999–2254.
- [3] Ben-Yakar, A., M.G. Mungal, and R.K. Hanson. 2006. Time evolution and mixing characteristics of hydrogen and ethylene transverse jets in supersonic crossflows. *Phys. Fluids*. 18(2):026101.
- [4] Kawai, S., and S.K. Lele. 2010. Large-eddy simulation of jet mixing in supersonic crossflows. *AIAA J*. 48(9):2063–2083.
- [5] Boles, J.A., J.R. Edwards, and R.A. Baurle. 2008. Hybrid LES/RANS simulation of transverse sonic injection into a Mach 2 flow. *AIAA Paper* 2008–622.
- [6] Won, S.H., I.S. Jeung, B. Parent, and J.Y. Choi. 2010. Numerical investigation of transverse hydrogen jet into supersonic crossflow using detached-eddy simulation. *AIAA J*. 48(6):1047–1058.
- [7] Shiryayeva, A.A. 2015. Features of the numerical method and the results of testing the program ZEUS-S3pp for three-dimensional combustion flow modelling. *TsAGI Works* 2735:220–246 (in Russian).
- [8] Ben-Yakar, A. 2000. Experimental investigation of mixing and ignition of transverse jets in supersonic crossflows. PhD Thesis. Stanford University.
- [9] Menter, F., C.J. Ferreira, T. Esch, and B. Konno. 2003. The SST turbulence model with improved wall treatment for heat transfer predictions in gas turbines. In: *International Gas Turbine Congress 2003, Tokyo*. IGTC2003-TS-059. 7 p.
- [10] Gritskevich, M.S., A.V. Garbaruk, J. Schütze, and F.R. Menter. 2011. Development of DDES and IDDES formulations for the $k-\omega$ shear stress transport model. *Flow Turb. Combust.* 88(3):431–449.
- [11] Shur, M.L., P.R. Spalart, M.K. Strelets, and A.K. Travin. 2015. An enhanced version of DES with rapid transition from RANS to LES in separated flows. *Flow Turb. Combust.* 95(4):709–737.
- [12] Suresh, A., H. Huynh. Accurate monotonicity-preserving schemes with Runge–Kutta time stepping. 1997. *J. Comput. Phys.* 136(1):83–99.
- [13] Molev, S.S. 2015. Improvement in modeling quality of unsteady processes when using an explicit scheme with fractional time stepping. *TsAGI Sci. J.* 46(8):783–806.
- [14] Sadovnichy, V., A. Tikhonravov, V. Voevodin, and V. Opanasenko. 2013. “Lomonosov”: supercomputing at Moscow State University. In: *Contemporary High Performance Computing: From Petascale toward Exascale*. Chapman & Hall/CRC Computational Science, 283–307.
- [15] Vyshinsky, V.V., and G.B. Sizykh. The verification of the calculation of stationary subsonic flows and the presentation of the results. 2019. *Math. Models Comp. Simul.* 11(1):97–106.
- [16] Vyshinsky, V.V., and G.B. Sizykh. 2019. Verification of the calculation of stationary subsonic flows and presentation of results. In: *Smart Modeling for Engineering Systems. GCM50 2018. Smart Innovation, Systems and Technologies*. 133:228–235.
- [17] Guseva, E.K. 2017. Analysis and evaluation of the effectiveness of methods that accelerate the transition to numerically resolved turbulence when using nonzonal hybrid approaches to the turbulent flow simulation. PhD Thesis. St. Petersburg State Polytechnic University (in Russian).